

G-47

ОБЪЕДИНЕННЫЙ
ИНСТИТУТ
ЯДЕРНЫХ
ИССЛЕДОВАНИЙ
ДУБНА



1234 / 2-74

1/11-74

E7 - 7688

**P.Gippner, K.-H.Kaun, W.Neubert, F.Stary,
W.Schulze**

**EXCITATION
OF KX-RAYS BY BOMBARDMENT
OF THICK SOLID TARGETS
WITH 150 MEV Xe IONS**

1974

ЛАБОРАТОРИЯ ЯДЕРНЫХ РЕАКЦИЙ

E7 - 7688

**P.Gippner, K.-H.Kaun, W.Neubert, F.Stary,
W.Schulze**

**EXCITATION
OF KX-RAYS BY BOMBARDMENT
OF THICK SOLID TARGETS
WITH 150 MEV Xe IONS**

Submitted to Nuclear Physics

Объединенный институт
ядерных исследований
БИБЛИОТЕКА

1. Introduction

The investigation of characteristic X-rays excited by the interaction of heavy ions with matter shows that even the K-shells of the colliding partners become ionized with high probability. The order of magnitude of the cross section values σ_K as well as its dependence on the ion energy, on the atomic numbers of the projectile (Z_1) and of the target (Z_2) raise the question about the mechanism of the K-shell ionization. For ions with the smallest atomic numbers Z_1 , such as protons and α -particles, the experimentally determined values of the total cross section σ_K are in good agreement with that for direct Coulomb ionization. ^{/1-6/} In the cases of incident energies fulfilling the adiabatic condition for inner shells and for ion-target combinations, for which the relation $Z_1 \ll Z_2$ is invalid, the dependence of the cross sections σ_K and σ_L on the experimental parameters is described in a qualitative way by the molecular orbital (MO) model ^{/2,7-12/}. By using this model, in ref. ^{/13/} the cross sections of K-shell ionization were calculated for the symmetric systems $C+C^+$, $N+N^+$, $O+O^+$ and $Ne+Ne^+$; in these cases one or more L-vacancies are brought in by the incident ions. Unfortunately, no quantitative calculations of the cross sections, which are to be expected from the MO model, are so far carried out for asymmetric systems or symmetric systems with $Z > 10$. In these cases direct experimental tests are currently impossible.

Some recent papers indicate that multiple collisions of ions in a target material lead to an asymmetric charge distribution, which contains also very high charge states ^{/14,15/}. Such high charge states may mainly result from outer shell ionization, but K-shell vacancies are not

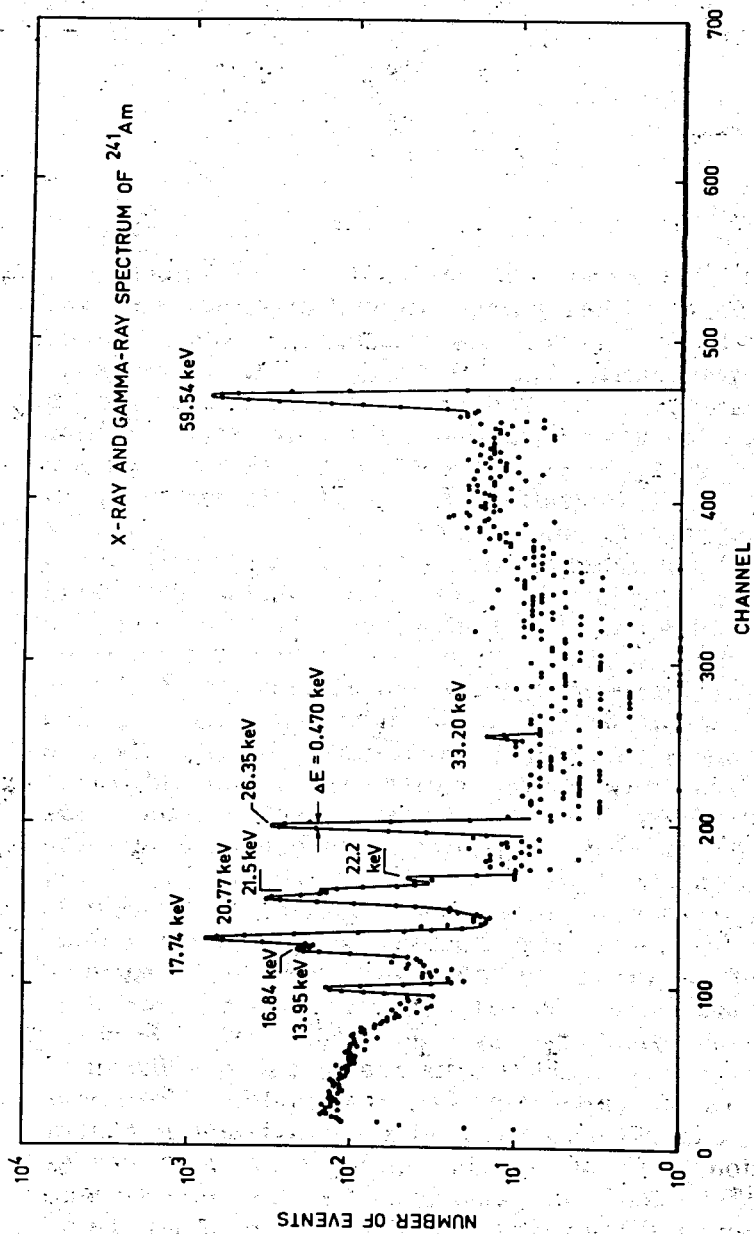


Fig. 1. X-ray and gamma-ray spectrum of ^{241}Am for energy calibration of the detector.

to be excluded. The concepts advanced so far on the formation of charge distributions by the interaction of ions in solids, give no statements on the mechanism of an individual collision. The K-shell vacancies, necessary for the production of KX-rays, may, therefore, originate from electron promotions as well as from any kind of direct process.

The investigations of K excitation cross sections, which are described in this paper, may contribute to clarify the mechanism of inner shell ionization in the case of high energies and heavy colliding ions.

2. Experimental Method

At the U-300 heavy ion cyclotron investigations of the emission of KX-radiation arising from the bombardment of different solid targets by $^{136}\text{Xe}^{9+}$ ions were carried out: The ion energy was 150 MeV., Currents of about 2×10^{10} ions per second were used. The principal experimental arrangement was described earlier ¹⁶. By means of a somewhat better focusing system, a focus of 6 mm diameter was achieved at the target location. The targets consisted of thick metallic foils covered by a frame of pure aluminium with an opening of $15 \times 15 \text{ mm}^2$. The parameters of the targets used are listed in table 1. The targets were exposed at an angle of 45° with respect to the beam direction, but the X-rays were measured perpendicularly to the beam direction. A grid of 0.1 mm tungsten wires, placed in front of the target, served to normalize the measured spectra to the equal quantities of incident ions.

For the detection of the KX-rays, a Si(Li) detector with a cooled FET preamplifier of 470 eV energy resolution at 26 keV X-ray energy was used. Figure 1 shows the LX- and γ -ray spectra of ^{241}Am , which was used for the energy calibration. The measurements were performed with a 1024-channel analyser. Figure 2 shows the X-ray spectrum obtained by bombardment of a Nb target.

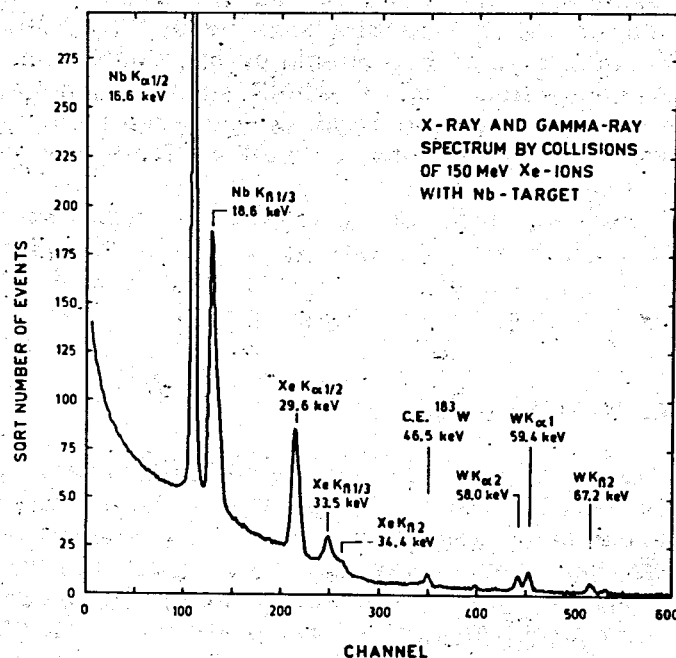


Fig. 2. The spectrum obtained by bombardment of a niobium target (and the tungsten grid) with 150 MeV Xe ions.

No X-rays of energies below 10 keV could be detected due to an electrically inactive layer inside the detector. Therefore the LX-radiation of the target materials could not systematically be investigated. As a result of the ionization of the inner shells of the tungsten nucleides, the characteristic KX-ray lines of tungsten were obtained together with the KX-radiation of Xe and the target materials (fig. 2). By means of the intensity of the tungsten X-rays, the normalization of the X-ray spectra to equal charges was carried out.

In order to obtain the absolute cross section values, the charge was measured without target foil. The number of KX-rays of the tungsten grid was compared with the charge of the ions passing through the grid to the Faraday cup. In this way any falsification of the charge measurement

Table 1
The types of targets used. The symbols designate the following: Z_1 and Z_2 , the atomic numbers of projectile and target, respectively; d , the effective target thickness in a 45° geometry; R the range, where 150 MeV Xe ions are losing an energy of 30 MeV ¹⁹⁷.

Target:	Z_2	Z_1/Z_2	$\frac{d}{\text{mg/cm}^2}$	$\frac{R}{\text{mg/cm}^2}$
Nb	41	1.32	34.4	0.95
Mo	42	1.29	26.3	0.97
Rh	45	1.20	19.4	1.00
Pd	46	1.17	26.4	1.01
Cd	48	1.12	9.1	1.04
In	49	1.10	28.1	1.05
Sn	50	1.08	11.3	1.07
Gd	64	0.84	10.8	1.28
Tb	65	0.83	5.4	1.30
Yb	70	0.77	8.2	1.39
Ta	73	0.74	27.2	1.48
Ir	77	0.70	18.4	1.50
Pt	78	0.69	15.7	1.51

due to changes in the charge of the Xe ions inside the target was avoided.

It is well known that inside the target materials the cross section of the KX-ray excitation changes very rapidly with the actual ion energy. In ref. /17/ it was assumed that the K_{α} -radiation of Cl ions of 120 MeV was emitted only in a thin target layer of about $100 \mu\text{g}/\text{cm}^2$. Other authors /18/ suggest an energy dependence of the KX-ray-radiation cross section to be proportional to $E(r)^5$. Together with the rapid decrease of the ion energy in solid materials, this causes X-ray emission only in the utmost layers of solid targets. For the evaluation of the cross sections we could not use the formula of Merzbacher and Lewis /1/, because it was impossible to vary the ion energy using the cyclotron, whereas the use of aluminium foils for decreasing the ion energy would give rise to very high uncertainties. Because for Xe ions no experimentally confirmed expression for the energy dependence of σ was known, we assumed that KX-radiation is produced only within a range R, in which the Xe ions are losing an energy of 30 MeV. Further we assume the KX-ray cross section to be constant within this range. The values of R evaluated using the tables of Northcliff and Schilling /19/ are listed in table 1.

The following corrections of the measured KX-ray intensities are to be made:

1. Self-absorption of the X-rays within the range R.
2. Excitation of Xe KX-radiation by the tungsten grid. Its portion was determined from a measurement without target, which was also normalized to the intensity of the characteristic KX-ray transitions of the tungsten grid.
3. In the case of the Gd, Tb and Yb targets, Coulomb-excited γ -ray transitions were obtained, whose inner conversion contributes to the target KX-ray intensity. Its portion was calculated from the intensity of the respective γ -ray lines and the known conversion coefficients. The rate of KX-radiation measured by our target-detector arrangement is given by the following relation:

$$N_m = \int n \sigma [E(r)] e^{-\mu r} dr, \quad (1)$$

where $E(r)$ is an ion energy dependent on the penetration depth along a stretched path inside the target; $\sigma[E(r)]$ is the cross section as a function of the ion energy. The value of $\bar{\sigma} = \sigma(E)$ averaged over the range R of the Xe ions and dependent only on the incident energy E is obtained from eq. (1) by making use of some correction factors

$$\bar{\sigma} = \frac{\mu N_{mc}}{n(1 - e^{-\mu R})} \cdot \frac{A}{\epsilon_{tot} \cdot M \cdot D}, \quad (2)$$

where N_{mc} is the measured and corrected number of KX-rays. In calculating the cross section $\sigma_K(Xe)$, the Xe K-radiation excited by the tungsten grid was subtracted. In calculating the cross sections σ_K (target) for Gd, Tb and Yb targets, the inner conversion of the Coulomb-excited γ -ray transitions was taken into account; μ is the target absorption coefficient for the K-radiation in cm^2/g ; R is the range listed in table 1; n is the number of target atoms per g; ϵ_{tot} is the total efficiency of the Si(Li) detector; D is the number of characteristic KX-rays of the tungsten grid acting as a normalization factor; M is a calibration factor obtained from the absolute charge measurement for Xe^{9+} ions; A is a correction factor for screening X-rays by the tungsten grid.

3. Experimental Results

In table 2 the evaluated cross section values $\sigma_{K\alpha}$ and $\sigma_{K\beta}$ for Xe and the investigated targets are summarized. Figures 3 and 4 show the dependence of these cross sections on the atomic number Z_2 of the target materials for a constant incident ion energy of 150 MeV. Figures 3 and 4 present additional cross section values, which we have measured by means of a Ge(Li) detector and which were referred to elsewhere /20/. These values have subsequently been corrected for self-absorption of KX-

Table 2
Cross sections $\sigma_{K\alpha}$ and $\sigma_{K\beta}$ for the excitation of KX -rays by bombardment of solid targets with 150 MeV Xe ions.

Target	Z_2	$\sigma_{K\alpha}(\text{Xe})$ cm^2	$\sigma_{K\alpha}(\text{target})$ cm^2	$\sigma_{K\beta}(\text{Xe})$ cm^2	$\sigma_{K\beta}(\text{target})$ cm^2
Nb	41	$(7.2 \pm 2.3) \cdot 10^{-25}$	$(5.6 \pm 3.2) \cdot 10^{-22}$	$(1.6 \pm 0.8) \cdot 10^{-25}$	$(4.3 \pm 2.2) \cdot 10^{-23}$
Mo	42	$(1.1 \pm 0.3) \cdot 10^{-24}$	$(3.8 \pm 1.5) \cdot 10^{-22}$	$(1.5 \pm 0.6) \cdot 10^{-25}$	$(3.4 \pm 1.3) \cdot 10^{-23}$
Rh	45	$(2.9 \pm 0.9) \cdot 10^{-24}$	$(2.4 \pm 0.6) \cdot 10^{-22}$	$(3.9 \pm 1.4) \cdot 10^{-25}$	$(3.2 \pm 1.0) \cdot 10^{-23}$
Pd	46	$(2.9 \pm 0.9) \cdot 10^{-24}$	$(2.0 \pm 0.7) \cdot 10^{-22}$	$(2.4 \pm 1.0) \cdot 10^{-25}$	$(2.0 \pm 0.8) \cdot 10^{-23}$
Cd	48	$(5.8 \pm 1.6) \cdot 10^{-24}$	$(1.6 \pm 0.5) \cdot 10^{-22}$	$(5.5 \pm 2.3) \cdot 10^{-25}$	$(1.9 \pm 0.7) \cdot 10^{-23}$
In	49	$(6.9 \pm 2.3) \cdot 10^{-24}$	$(1.2 \pm 0.3) \cdot 10^{-22}$	$(7.5 \pm 2.2) \cdot 10^{-25}$	$(1.3 \pm 0.5) \cdot 10^{-23}$
Sn	50	$(9.4 \pm 2.4) \cdot 10^{-24}$	$(9.4 \pm 3.0) \cdot 10^{-23}$	$(6.9 \pm 2.1) \cdot 10^{-25}$	$(1.1 \pm 0.5) \cdot 10^{-23}$
Gd	64	$(2.1 \pm 0.8) \cdot 10^{-23}$	$(3.3 \pm 2.4) \cdot 10^{-24}$	$(2.7 \pm 1.2) \cdot 10^{-24}$	$(7.2 \pm 5.1) \cdot 10^{-25}$
Tb	65	$(1.6 \pm 0.9) \cdot 10^{-23}$	$(4.7 \pm 4.4) \cdot 10^{-24}$	$(2.0 \pm 1.3) \cdot 10^{-24}$	$(1.3 \pm 1.4) \cdot 10^{-24}$
Yb	70	$(2.8 \pm 1.0) \cdot 10^{-23}$	$(2.4 \pm 2.0) \cdot 10^{-24}$	$(3.3 \pm 1.6) \cdot 10^{-24}$	$(7.9 \pm 7.4) \cdot 10^{-25}$
Ra	73	$(2.9 \pm 0.8) \cdot 10^{-23}$	$(1.9 \pm 1.0) \cdot 10^{-24}$	$(3.4 \pm 1.2) \cdot 10^{-24}$	$(4.0 \pm 2.1) \cdot 10^{-25}$
Ir	77	$(1.5 \pm 0.5) \cdot 10^{-23}$	$(5.6 \pm 3.5) \cdot 10^{-25}$	$(2.1 \pm 0.8) \cdot 10^{-24}$	$(2.8 \pm 2.4) \cdot 10^{-25}$
Pt	78		$(5.9 \pm 3.5) \cdot 10^{-25}$		$(1.7 \pm 0.9) \cdot 10^{-25}$

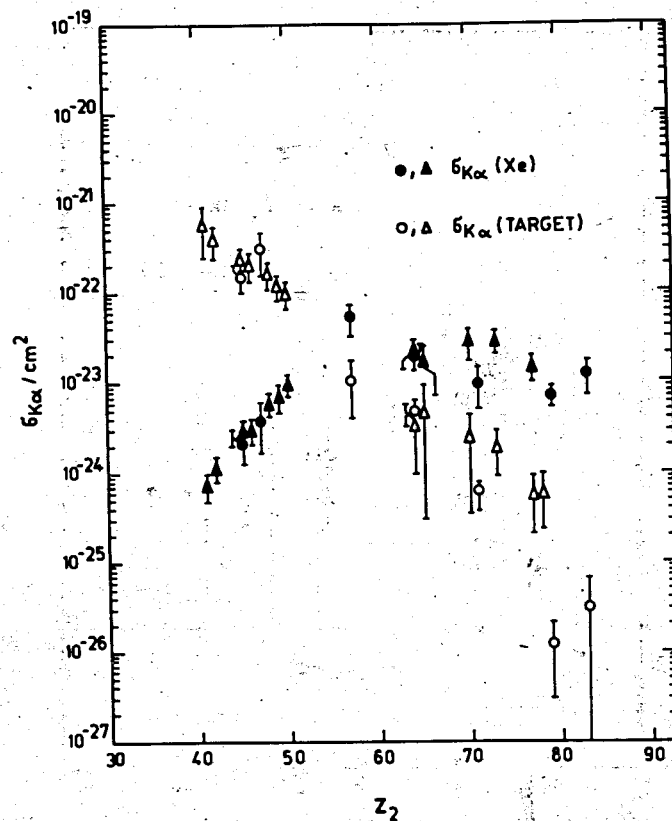


Fig. 3. Absolute cross sections $\sigma_{K\alpha}(\text{Xe})$ and $\sigma_{K\alpha}(\text{target})$ as a function of the atomic number Z_2 of the target material. The values denoted by the symbols \blacktriangle and \triangle are measured by means of a Si(Li) detector, the values denoted by \bullet and \circ we have obtained by a Ge(Li) detector and referred elsewhere /20/.

rays within the range R. In the calculations of the errors $\Delta\sigma_K$ given in table 2 and figs. 3 and 4, only the errors in the peak areas N_{mc} and D, the absorption coefficients μ and the ranges R have been taken into account. These values are uncertain from target to target and effect the

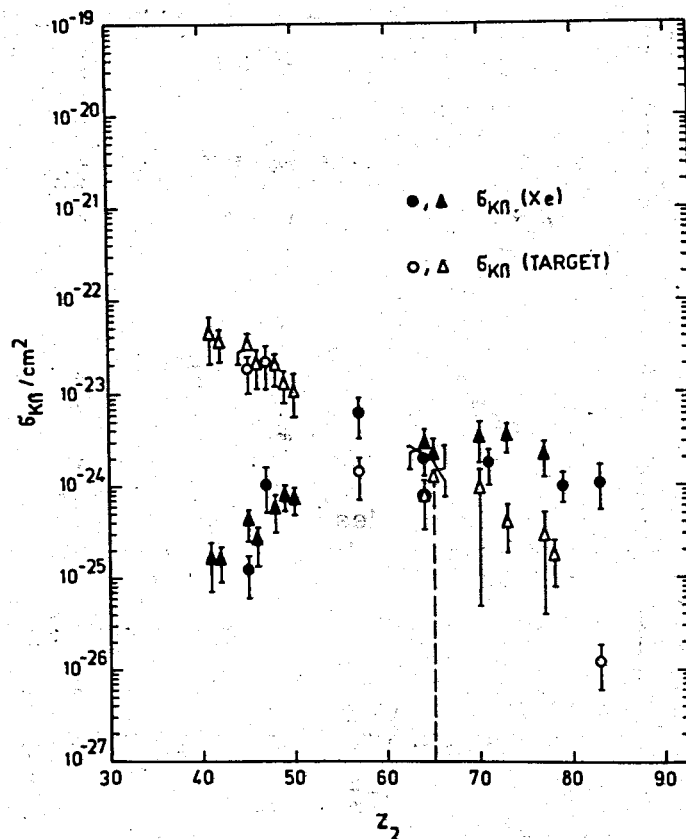


Fig. 4. Absolute cross sections $\sigma_{K\beta}(Xe)$ and $\sigma_{K\beta}(\text{target})$ as a function of the atomic number Z_2 . For meaning of the symbols see caption of fig. 3.

relative positions of several points in figs. 3 and 4. The neglected errors of the detector efficiency ϵ_{tot} and the factors M and A influence to an equal extent all the points of figs. 3 and 4, i.e., only the absolute cross section values. The account of the systematical errors $\Delta\epsilon_{\text{tot}}$, ΔA and ΔM increases the relative errors $\Delta\sigma_K/\sigma_K$ by 20%.

4. Discussion

The experimental facts described in section 3 may be explained qualitatively in terms of the MO model ^{/9,11/}. In principle, this model is applicable to our experiment, because the adiabatic condition $v \ll u$ is fulfilled for every target and the quantum numbers $n=1, 2$ and 3. For instance, for the M-shell of ^{45}Rh the condition $v/u \approx 0.3$ is valid. This ratio decreases with increasing Z of the target and decreasing quantum numbers n . The time required for penetration of the K- and L-shells of the collision partners is of the order of 10^{-18} s, whereas for solid targets the time between two collisions amounts to about 10^{-17} s. Vacancies in the M, L- and K-shells of Xe have life-times of 10^{-14} , 10^{-15} and 10^{-16} s, respectively ^{/21/}. They are, therefore, able to survive several collisions and to give rise to the emission of characteristic X-rays after the particles have been separated. For an incident energy of 150 MeV the mean charge state of Xe ions is about $\bar{q}=28$ (refs. ^{/22,23/}). It may, therefore, be assumed that after some collisions with the outermost target layer a large number of Xe ions contain vacancies in the 3d-shell. Figure 5a and 5b show the correlation schemes for the system $^{45}\text{Rh} + ^{54}\text{Xe}$ and $^{64}\text{Gd} + ^{54}\text{Xe}$, respectively. As can be seen from these figures for a target with $Z_2 < 54$, according to the MO model, vacancies may get across the 3d δ -term to the quasiatom with $Z = 99$ and therefrom into the 2p-shell of the Xe ion. Filling these vacancies by outer electrons causes LX-rays of Xe. If, however, during the lifetime of the 2p vacancy a further collision takes place, the vacancy may be transferred into the 1s-shell of the Rh atom. Multiple collisions lead to the excitation of KX-radiation of Rh. If the atomic number Z_2 nearly agrees with that of Xe, i.e., both the target and projectile have almost equal K binding energies, the 1s-electrons of Xe may also be promoted into the higher states with high probability resulting in a large cross-section $\sigma_K(Xe)$ (fig. 3). This mechanism explains qualitatively that for $Z_2 < 54$ the lighter collision partner becomes preferably K ionized.

Similar arguments are used in paper /24/ to explain the KX -radiation of Ne ions, originating from bombardment of an Ar gas target. For both types of collisions, only a very low rate determined by the ratio of the particle densities is to be expected. Neglecting the backward diffusion of the ions, in the collisions of Xe with Xe an accumulation effect should be observed. At the end of a 30 min. irradiation, the ion current leads to one Xe + Xe collision, compared with 10^5 of Gd + Xe collisions. Experimentally, no change in the intensity ratio between the target and Xenon radiation has been found with an accuracy of a few percent for an irradiation period of 1.5 hours. For $Z_2 > 54$ the origin of the target KX -radiation could be explained as being due to recoils of L ionized target atoms. During the formation of quasimolecules with other target atoms, K -shell vacancies may be produced in the symmetric colliding system. In this way the formation of target KX -rays may in principle be understood also for targets with $Z_2 > 54$. In the framework of the MO model Meyerhof /25/ has tried to explain the production of K vacancies also for asymmetric systems. On the basis of the charge transfer theory of Demkov /26/, he provides an explanation of K ionization of the higher Z partner by suggesting that, after $2p\sigma - 2p\pi$ electron promotion by rotational coupling at small internuclear distances (fig. 5b), a further charge transfer can take place between the $1s\sigma$ and $2p\sigma$ terms by radial coupling. For the probability $w(x)$ of vacancy transfer from the $2p\sigma$ orbital (lower Z) to the $1s\sigma$ orbital (higher Z) Meyerhof gives the relation

$$w(x) = 1 / (1 + e^{2|x|}), \quad (3)$$

where

$$x = \pi(I_1 - I_2) / [8m_e I]^{1/2} v_1. \quad (4)$$

Expression (3) is valid if the radial coupling acts only in the exit channel. In formula (4) I_1 and I_2 denote the K binding energies for the projectile and target,

respectively, v_1 is the projectile velocity, m_e the electron mass and I a mean value of the K binding energies in the following form: $I^{1/2} = (I_1^{1/2} + I_2^{1/2})/2$. The probability w is related to the cross sections $\sigma_K(H)$ and $\sigma_K(L)$ for ionization of the K-shells in the higher- and lower- Z partner by the expression /25/

$$w = \sigma_K(H) / (\sigma_K(H) + \sigma_K(L)). \quad (5)$$

Figure 6 shows the probabilities w , as they can be evaluated from our experimental results (table 2). For $x > 0$, where $Z_1 > Z_2$, i.e., the Xe ions are the higher-Z partners, the experimental values approximate the theoretical expression (3) satisfactorily. In these cases the radial coupling can account for the ionization of the Xe K -shell in the framework of the MO model. However, for $x < 0$, where $Z_1 < Z_2$, i.e., the target atoms are the higher- Z partners, Meyerhof's suggestions can not explain our experimental results. Since the measured values are located above the theoretical curve of formula (3), we assume that the recoil of target atoms contributes strongly to the cross sections $\sigma_K(H)$. In the case of $Z_1 > Z_2$, this recoil may only magnify the values $\sigma_K(L)$ and may, therefore, explain the fact that the experimentally found values of w are somewhat smaller than the theoretical ones.

For the minimum distance between the colliding particles the relation

$$R_{\min} = \frac{\epsilon^2 Z_1 Z_2}{E_{\text{lab}}} \cdot \frac{M_1 + M_2}{M_2} \quad (6)$$

is valid. Provided that the energy E_{lab} of the Xe ions is constant, R_{\min} increases with increasing Z_2 . This effect leads to a decrease in the following ionization cross sections:

a) $\sigma_L(Xe)$ for L ionization of the Xe ions in collisions with target atoms.

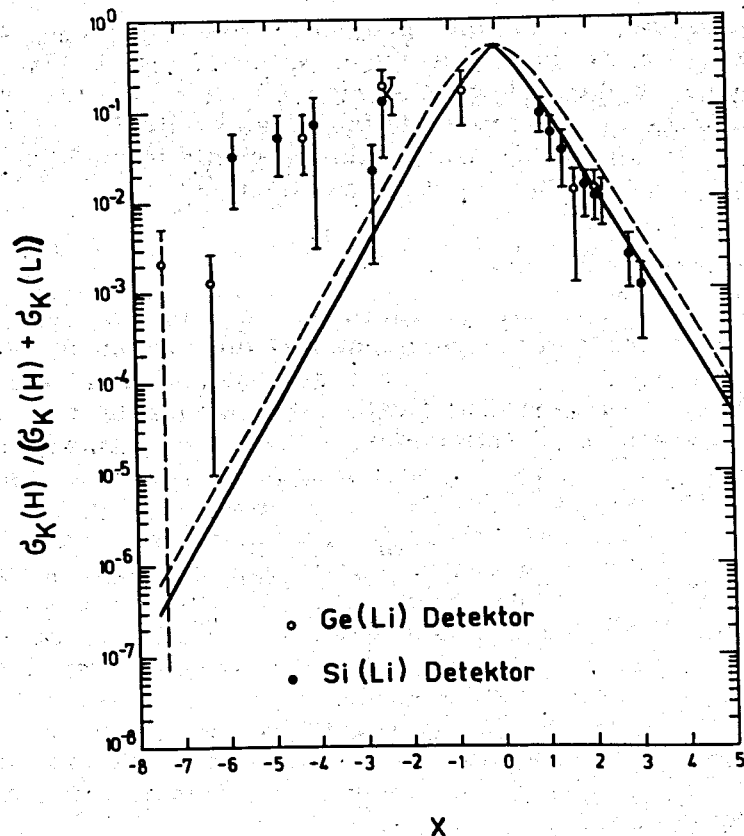


Fig. 6. Comparison of the experimental results with the expression $w(x)$ for the $2p\sigma$ vacancy transfer to the $1s\sigma$ orbital of the higher Z partner. The solid line corresponds to the radial coupling only in the exit channel, the dashed line to the coupling in both the entrance and the exit channels.

b) σ_K (target) for K ionization of recoiled target atoms in collisions with target atoms. This leads to a decrease in σ_K (target) with increasing Z_2 (figs. 3 and 4).

Summary

In the bombardment of several targets with 150 MeV Xe ions the absolute cross sections $\sigma_K(\text{Xe})$ and $\sigma_K(\text{target})$ have been measured. The discussion of the experimental results shows that for $Z_2 < 54$ the MO model is capable of explaining the cross section ratios $\sigma_K(H) / (\sigma_K(H) + \sigma_K(L))$ in a quantitative way. Moreover, from this model the cross section σ_K of the projectile may be expected to show a maximum in the case of a symmetric collision system $Z_1 = Z_2$. For Xe ions the height and position of this maximum may be interpolated from the measured cross section curves $\sigma_{K\alpha}(\text{Xe})$ and $\sigma_{K\beta}(\text{Xe})$. For $Z_2 > 54$, the KX-radiation of Xe and the target materials are no longer understood on the basis of multiple collisions of Xe ions with target atoms. An explanation of the Xe radiation with the help of the collisions of Xe ions with implanted Xe atoms seems improbable. For a possible explanation of the target radiation, use was made of target recoil collisions. The Z_2 dependence of $\sigma_K(\text{Xe})$ and $\sigma_K(\text{target})$ for $Z_2 > 54$ gives a hint at the formation of quasimolecules in this case too.

The authors would like to thank Academician G.N. Fleurov for his interest in the problem, Drs. A.I. Kalinin and H. Ulrich for installing the Si(Li) detector, the heavy-ion cyclotron staff for their cooperation and Mrs. I. Schulze for her technical help.

References

1. E. Merzbacher and H.W. Lewis. Handbuch der Physik, ed. by E. Flügge, Springer-Verlag Berlin, 1958, Vol. 34, p. 166.
2. W. Brandt and R. Laubert. Phys. Rev. Lett., 24, 1037 (1970).
3. J.M. Hansteen and O.P. Mosebekk. Z. Phys., 234, 281 (1970).
4. R.L. Watson, C.W. Lewis and J.B. Natowitz. Nucl. Phys., A154, 561 (1970).
5. J.M. Hansteen and O.P. Mosebekk. Contr. to the

Proceedings of the International Conf. on Inner Shell Ionization Phenomena, Atlanta, 1972.

6. O.N.Jarvis and C.Whitehead. Phys.Rev., A5, 1198 (1972).
7. W.Lichten. Phys.Rev., 164, 131 (1965).
8. H.J.Specht. Z. Phys., 185, 301 (1965).
9. U.Fano and W.Lichten. Phys.Rev.Lett., 14, 627 (1965).
10. J.Macek. Phys.Rev.Lett., 28, 1298 (1972).
11. M.Barat and W.Lichten. Phys.Rev., A6, 211 (1972).
12. H.O.Lutz; J.Stein, S.Datz and C.O.Moak. Phys.Rev.Lett., 28, 8 (1972).
13. J.S.Briggs and J.H.Macek. J.Phys., B6, 982 (1973).
14. C.A.Ryding, A.B.Wittkower and P.H.Rose. Phys.Rev., A3, 1658 (1971).
15. H.D.Betz. Rev.Mod.Phys., 44, 465 (1972).
16. U.Hagemann, W.Neubert, W.Schulze and F.Stary. Nucl.Instr. and Meth., 96, 415 (1971).
17. H.W.Schnopper, A.R.Sohval, H.D.Betz, J.P.Delvaile, K.Kalata, K.W.Jones and H.E.Wegner. Contr. to the Proceedings of the International Conf. on Inner Shell Ionization Phenomena, Atlanta, 1972.
18. W.E.Meyerhof. Private communication.
19. L.C.Northcliff and R.F.Schilling. Nucl. Data Tables, A7, 233 (1970).
20. P.Gippner, K.H.Kaun, W.Neubert, F.Stary and W.Schulze. JINR, E7-7214, Dubna, 1973.
21. H.R.Rosner and C.P.Bhalla. Z. Phys., 231, 347 (1970).
22. V.S.Nikolajev and I.S.Dmitriev. Phys.Lett., 28A, 277 (1968).
23. I.A.Shelayev, V.S.Alfeev, B.A.Zager, S.I.Kozlov; I.V.Kolesov, A.F.Linev, V.N.Melnikov, R.Ts.Oganesyan, Yu.Ts.Oganesyan, V.A.Chugreev. JINR, P9-6062, Dubna, 1971.
24. H.Tawara and J.Kistemaker. Phys.Lett., 41A, 287 (1972).
25. W.E.Meyerhof. Phys.Rev.Lett., 31, 1341 (1973).
26. Yu.N.Demkov. JETP, 18, 138 (1964).

Received by Publishing Department
on January 24, 1974.